Electrically Fueled Active Supramolecular Materials

Serxho Selmani^{1,2} Eric Schwartz^{1,2}, Justin T. Mulvey^{1,3}, Hong Wei^{1,3}, Adam Grosvirt-Dramen^{1,4}, Wyeth Gibson^{1,2}, Allon I. Hochbaum^{1,2,3,4,5}, Joseph P. Patterson^{1,2,3}, Regina Ragan^{1,3}, Zhibin Guan^{1,2,3,4,6}*

¹Center for Complex and Active Materials, University of California, Irvine, Irvine, California 92697, United States. ²Department of Chemistry, University of California, Irvine, Irvine, California 92697, United States. ³Department of Materials Science and Engineering, University of California, Irvine, Irvine, California 92697, United States. ⁴Department of Chemical and Biomolecular Engineering, University of California, Irvine, Irvine, California 92697, United States. ⁵Department of Molecular Biology and Biochemistry, University of California, Irvine, Irvine, California 92697, United States. ⁶Department of Biomedical Engineering, University of California, Irvine, Irvine, California 92697, United States.

ABSTRACT: Fuel-driven dissipative self-assemblies play essential roles in living systems, contributing both to their complex, dynamic structures and emergent functions. Several dissipative supramolecular materials have been created using chemicals or light as fuel. However, electrical energy, one of the most common energy sources, has remained unexplored for such purposes. Here we demonstrate a new platform for creating active supramolecular materials using electrically fueled dissipative self-assembly. Through an electrochemical redox reaction network, a transient and highly active supramolecular assembly is achieved with rapid kinetics, directionality, and precise spatiotemporal control. As electronic signals are the default information carriers in modern technology, the described approach offers a potential opportunity to integrate active materials into electronic devices for bioelectronics applications.

INTRODUCTION

Fuel-driven dissipative supramolecular assemblies in biology, such as actin filaments and microtubules contribute to the formation of complex, dynamic structures in living organisms and give rise to emergent functions such as motility, homeostasis, self-healing, and camouflage. 1,2 Such outof-equilibrium active supramolecular systems in living systems exhibit important emergent properties that are controlled spatiotemporally by the kinetics of fuel consumption³. Over the past decade, several synthetic dissipative assembly systems have been developed using chemicals⁴⁻⁷ or light8-10 as the major fuel sources. Chemical fuels such as alkylating agents⁴, carbodiimides^{11,12}, ATP/GTP¹³⁻¹⁷, and oxidants¹⁸⁻²⁰, have been used to drive dissipative assemblies of various building blocks including organic molecules4,11,12,19,21, peptides11,22,23, DNAs17,24, and nanoparticles²⁵. Light has also been used to drive dissipative assembly of small molecules^{26,27}, proteins⁹, and particles^{8,28}. These two main types of fueled active material systems complement each other with their respective advantages and limitations^{5,10}. Chemical fuels are versatile and have relatively high efficiency in generating the activated state, but face the challenge of generating waste in closed systems and are inherently limited in achieving spatiotemporal control of the dynamic assemblies⁵. Light, on the other hand, is a cleaner fuel with no waste generation and can be delivered spatiotemporally to control the assembly process; however it is limited in penetration depth and has lower efficiency in generating the activated state¹⁰.

Another major energy form, electrical energy, has remained mostly unexplored for fueling active supramolecular

assembly. Electrical energy offers several advantages as a fuel: it is readily available, clean, and can be modulated spatiotemporally. Electrical fields have been used to actuate electroactive polymers²⁹ and liquid crystalline materials³⁰, control particle assembly³¹, and power particle motions through various forms of electrostrictive hydrodynamics³². Electric potential has also been shown to polymerize organic monomers^{33,34} and modulate supramolecular interactions^{35,36}. Nevertheless, no prior study has reported electrically fueled (e-fueled) dissipative self-assembly of active supramolecular materials in bulk solution.

RESULTS AND DISCUSSION

Designing e-Fueled Dissipative Assembly System. To achieve our e-fueled dissipative self-assembly system, we designed an electrochemical redox reaction network that converts a cysteine derivative (CSH) into its corresponding cystine derivative (CSSC), which self-assembles into fibers (Fig. 1a)37. Ferrocyanide ([Fe(CN)6]4-), a safe and biologically tolerated reagent³⁸, was used as a homogeneous electrocatalyst because it could be easily oxidized electrochemically to ferricyanide ($[Fe(CN)_6]^{3-}$), which could further oxidize cysteine to the cystine³⁹. The disassembly half of the redox reaction network was accomplished by using chemical reductant dithiothreitol (DTT). When a positive electric potential is applied to the working electrode, [Fe(CN)₆]⁴⁻ near the electrode surface is oxidized to [Fe(CN)₆]³⁻ via electron transfer to the electrode, which subsequently oxidizes CSH into CSSC initiating fiber growth from the surface (Fig. 1b). As the potential is removed, DTT present in solution reduces CSSC back to CSH, resulting in the spontaneous dissolution of the fibers.

To test the feasibility of our design, we first confirmed that $[Fe(CN)_6]^{4-}$ acts as a homogeneous electrocatalyst for CSH

oxidation. Cyclic voltammograms (CV) of $[Fe(CN)_6]^{4-}$ and CSH in aqueous buffer (Fig. 1c) shows that the former was easily and reversibly

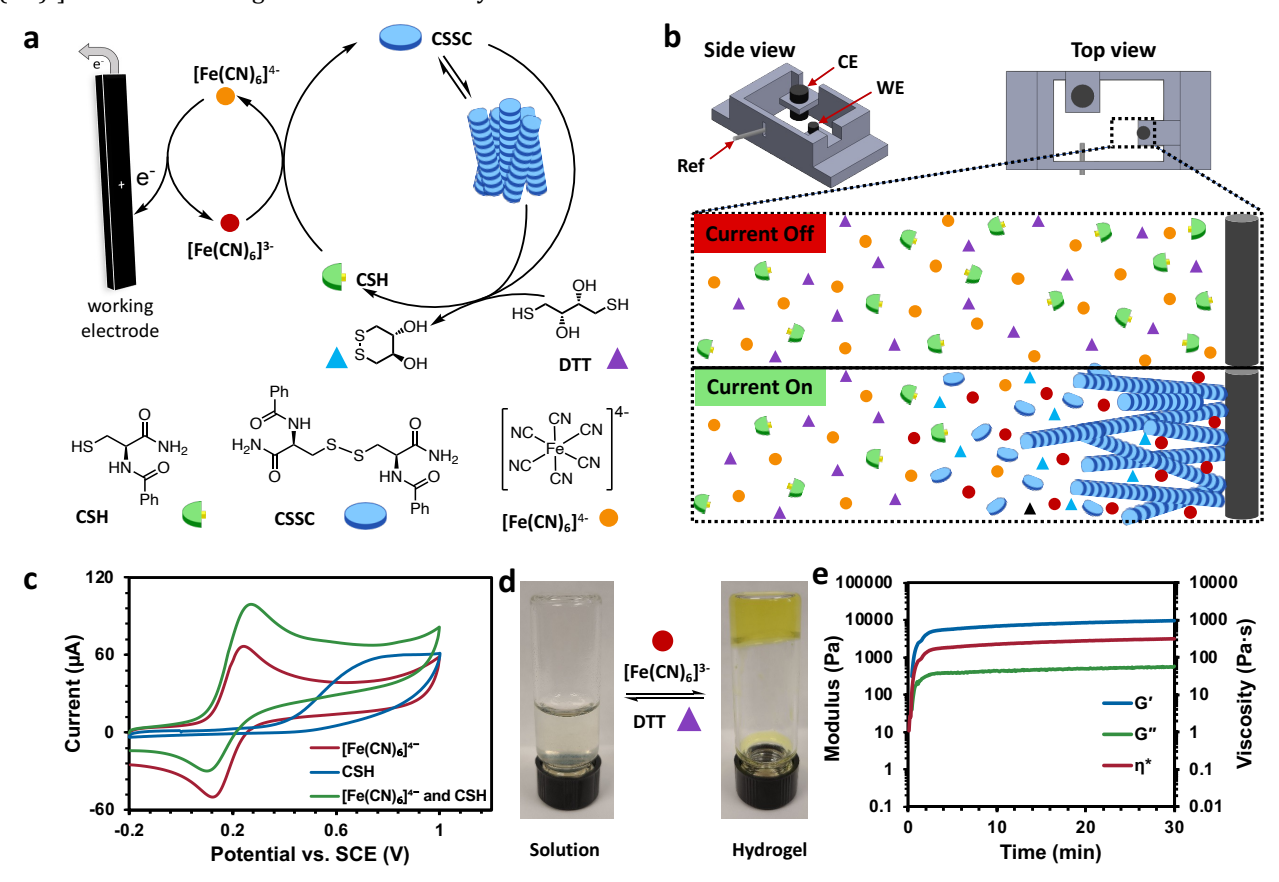


Figure 1. Design of electrically fueled active materials. (a) Schematic representation of the dissipative self-assembly process fueled by electricity. (b) Side and top view of the electrochemical cell used in the study (CE = glassy carbon counter electrode, WE = glassy carbon working electrode, Ref = silver wire pseudo-reference electrode), and schematic representation of species distribution in the cell when current is turned on and off. (c) Cyclic voltammogram showing electrocatalytic oxidation of CSH by ferricyanide ([Fe(CN)₆]³⁻) generated *in situ*. (d) Images showing the reversible fiber assembly and dissolution upon addition of [Fe(CN)₆]³⁻ or DTT to the solution ([CSH]₀ = 5.0 mM, pH = 8). (e) Rheology measurements showing the formation of hydrogel upon addition of [Fe(CN)₆]³⁻ to CSH solution (same condition as d).

oxidized with a $E_{1/2}$ = 200 mV vs. Ag/Ag⁺, whereas CSH was oxidized at 600 mV vs. Ag/Ag⁺ irreversibly. When $[Fe(CN)_6]^{4-}$ was added to CSH solution, the CV became electrochemically irreversible as shown by the cathodic current being significantly smaller in magnitude than the anodic current, indicating that $[Fe(CN)_6]^{4-}$ was participating in the electrocatalytic oxidation of CSH. The kinetics for the redox reactions involved in the system were quantified through a combination of stopped flow UV-Vis spectroscopy and ultra-performance liquid chromatography (UPLC) (see SI for details). Based on the kinetics, we demonstrated that $[Fe(CN)_6]^{3-}$ could oxidize CSH to form CSSC gel, which could be dissolved by DTT, as was visualized by vial inversion (Fig. 1d) and confirmed by rheology (Fig. 1e, Fig. S14, Fig. S15).

e-Fueled Transient and Directional Assembly. To demonstrate e-fueled dissipative self-assembly, we fabricated a custom glass-bottom, three-electrode bulk electrochemical cell (Fig. 1b, Fig. S1) in which e-fueled dissipative assembly could be monitored *in situ* using confocal laser

scanning microscopy (CLSM). We screened experimental parameters to determine conditions for fast fiber growth and dissolution. We began by identifying the minimal [CSH]₀ and maximal [DTT]₀ that allowed for fiber formation at relatively low potential (<1 V vs Ag/Ag+). Then, several experimental parameters were iteratively varied, including pH, [CSH]₀, [DTT]₀, and electrical current. As expected, increasing the current led to faster and more vigorous fiber growth (Fig. S3) while increasing [DTT]0 accelerated the dissolution (Fig. S4). The kinetics of fiber dissolution were pH dependent, with higher pH resulting in faster dissolution (Fig. S5), in agreement with previous studies¹⁹. The concentration of CSH within the range of 2 to 5 mM did not significantly impact growth and dissolution kinetics (Fig. S6). On the basis of these observations, the dissipative self-assembly was conducted in a pH 8 buffer with 2.5 mM CSH, 20 mM DTT. 150 mM ferrocyanide, and 25 μ M Nile red (as an intercalation dye for CLSM)19 by applying a potential of 430 mV between the glassy carbon working electrode and silver wire pseudo reference electrode (Fig. 1b).

Shortly after applying the potential, fibers began to grow directionally perpendicular to the surface of the working electrode which continued to grow outwards when the potential was maintained (Fig. 2a, SI Movie 1). When the current was turned off at 5 minutes, the fibers began to disassemble and eventually disappear. The fluorescence disappearance suggests that the DTT reduction-induced disassembly may

proceed both through monomer dissociation from the fiber ends and erosion from the fiber side surfaces. A combination of fiber shrinking from the ends and erosion from the side surfaces may contribute to the observed fluorescence change during dissipation. The fiber morphology of the efueled assembly was confirmed by cryo-

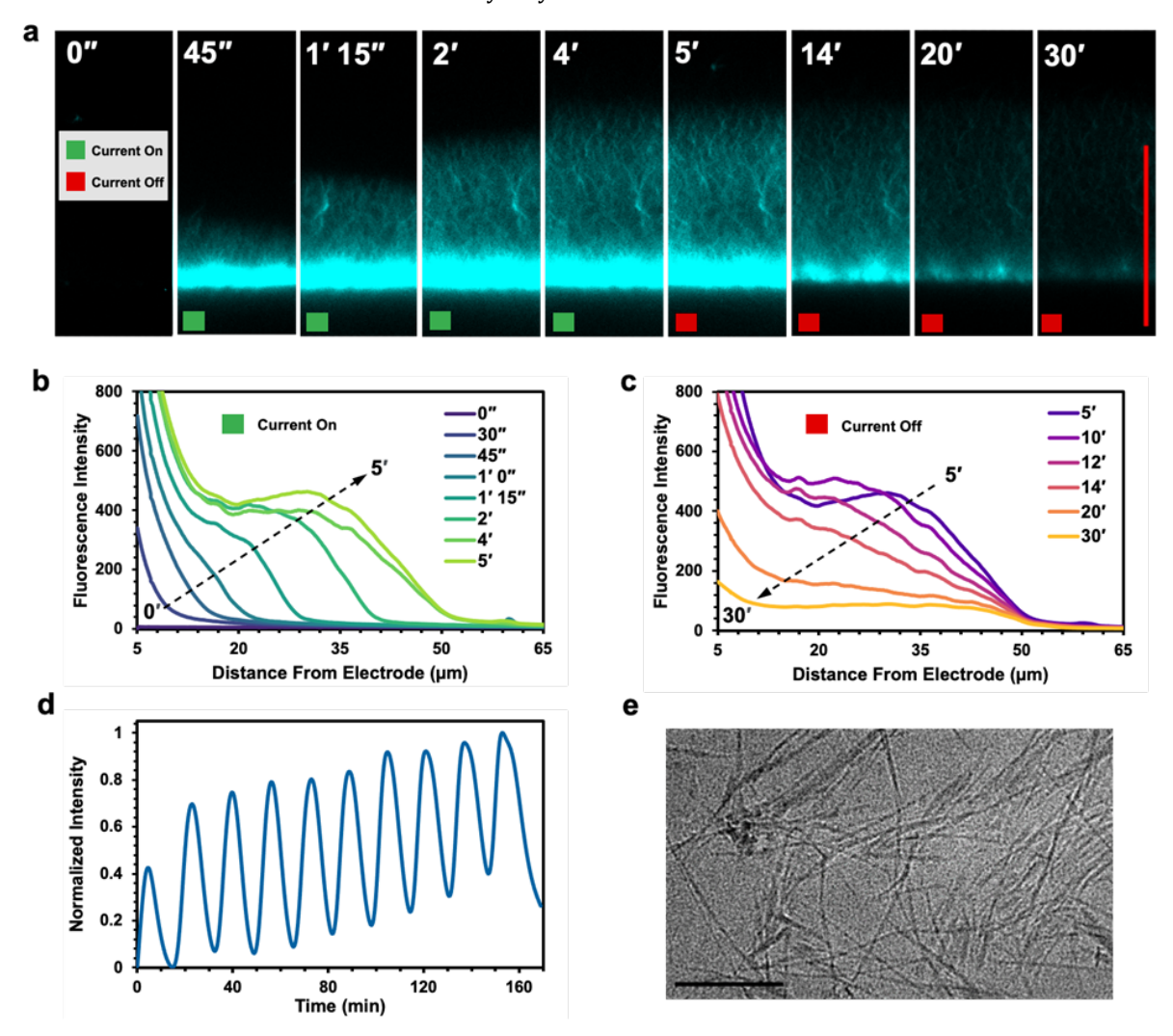


Figure 2. e-Fueled transient supramolecular assembly. (a) CLSM snapshots showing directional fiber growth when current was applied (green square), and dissolution when current was turned off (red square) (pH 8, [CSH] $_0$ = 2.5 mM, [DTT] $_0$ = 20 mM, [[Fe(CN) $_6$] $_1$ -] $_0$ = 150 mM, Scale bar = 50 μ m, 175 % hue saturation, electrode at bottom). (b, c) Fluorescence intensity at varying distances from the electrode surface observed over time during fiber growth with current on (b) and dissolution with current off (c). (d) Ten cycles of fiber growth and dissipation by repetitively switching current on and off (600 mV vs Ag/Ag+ for 16 sec followed by 24 min current off, under same condition as a). (e) A cryo-TEM micrograph of self-assembled fibers formed by e-fueled assembly (Scale bar = 200 nm).

TEM imaging, showing fibers with average diameters ~ 12 nm and average length ~ 412 nm (Fig. 2e, Fig. S17). The fibers were observed to stack and coil together creating larger micron sized assemblies (Fig. S16). The fluorescence histograms of the image reveal that during the fiber growth with the current on, they grew outwards as a front while steadily increasing in fluorescence intensity throughout the body of the gel (Fig. 2b). Conversely, when the fibers began to disassemble with the current off, the fiber front gradually receded toward the electrode while the fluorescence intensity dropped across the gel as a whole (Fig. 2c). This is

consistent with the fact that as the ferricyanide ($[Fe(CN)_6]^{3-}$) is generated at the electrode, it transports away from the electrode and oxidizes CSH into CSSC at the fiber front, enabling fibers to grow outwards (Fig. 1b). Upon depletion of the ferricyanide when current is turned off, the DTT in the bulk solution will diffuse back into the gel, initially reducing fibers at the front but then the body of the gel. The electrochemical generation of $[Fe(CN)_6]^{3-}$ results in the formation of two regions in our system. The region closest to the electrode is rich in oxidant as the generated $[Fe(CN)_6]^{3-}$ depletes the DTT, and the remainder of the bulk solution is a

reducing region rich in DTT. The gel was grown as far as 1.5 mm from the electrode surface through continual application of current for 30 minutes (SI Movie 2). Furthermore, the transient fibers could be grown and dissolved repetitively by turning the current on and off (Fig. 2d). These experiments clearly demonstrate the transient nature, directional growth, and precise temporal control of the e-fueled dissipative self-assembly.

Several control experiments were conducted to confirm that there was no appreciable photobleaching under experimental conditions (SI Movie 3 & 5) and the observed fluorescence changes were due to intercalation of the Nile Red dye into self-assembled fibers rather than simple electrochemical activation or physical attraction of the dye (SI Movie 4 & 5). Without DTT in the solution, the static fibers formed by electrochemical oxidation of CSH did not show any appreciable change in fluorescence intensity over one hour period after the current was turned off (SI Movie 3), indicating no significant photobleaching under experimental conditions. In the full system, the observed fluorescence decreases with the current off (Fig. 1a, SI Movie

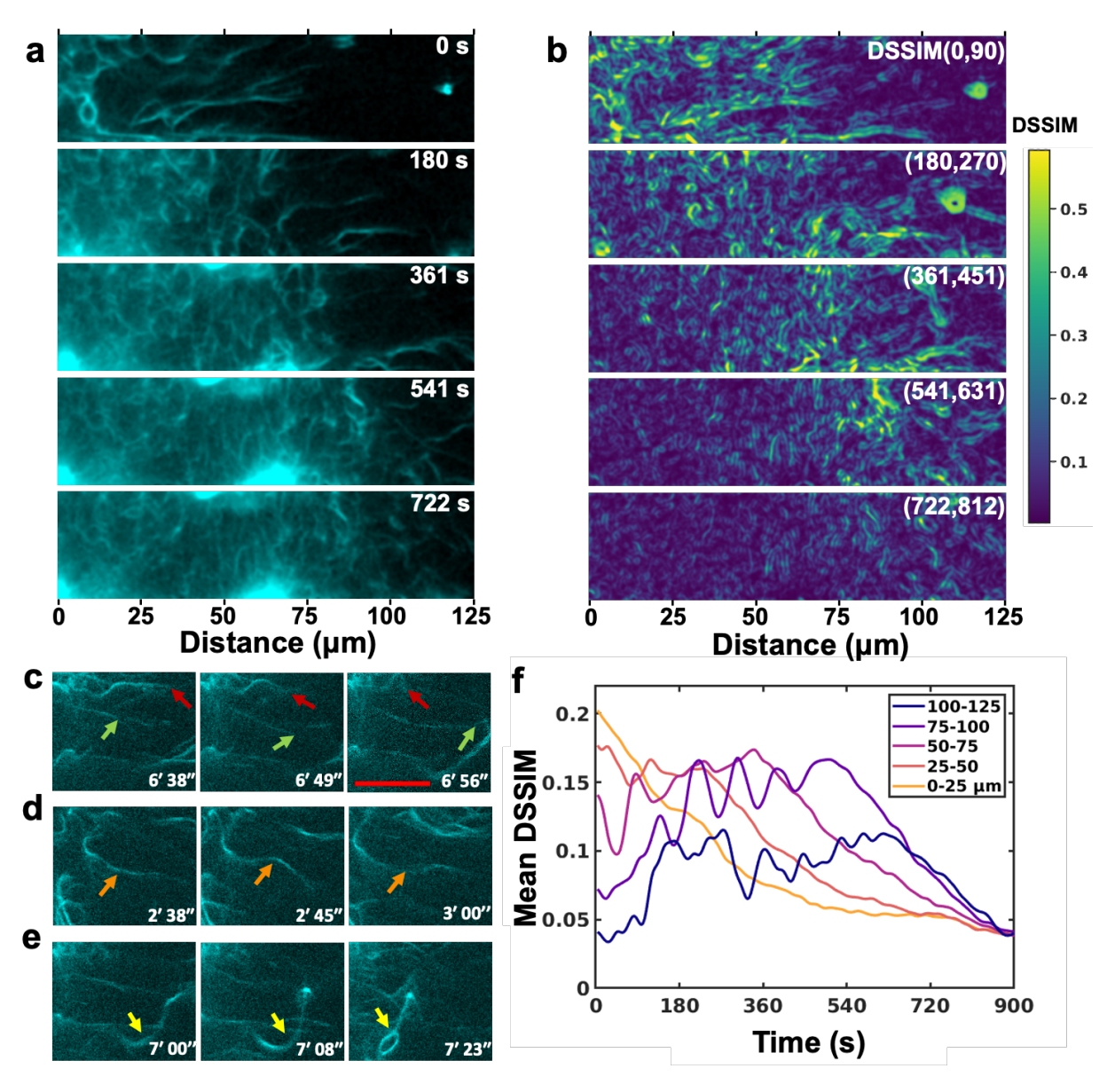


Figure 3. Active dynamic self-assembly fueled by electricity. (a) Processed CLSM snapshots highlighting the high dynamics for self-assembly at the gel front (details in SI). (b) Structural dissimilarity frame series generated by calculating the DSSIM of CLSM frames taken 90 s apart. Bright pixels represent regions of high structural dissimilarity between local areas in frames of comparison, which corresponds to fiber dynamics. (c-e) Snapshots showing different active fiber movements: simultaneous fiber growth and shrinkage (c, green arrow for growing fiber and red for shrinking), waving (d), and curling/looping (e) (CLSM images rendered with gamma = 0.45 and 150% hue saturation for fiber visualization). (f) Mean DSSIM in each region seen in b. (The working electrode for a-e is out of frame on the left. Scale bar = $20 \mu m$ for c-e)

1) was indeed due to fiber disassembly caused by DTT induced reduction of CSSC. In the absence of the CSH

precursor in the solution, no fibers were observed at all despite that an electrical potential ($600\ mV$) was repetitively

applied to the system (SI Movie 4), confirming that electrochemical oxidation of CSH to CSSC led to the fiber assembly. Lastly, without ferricyanide ([Fe(CN)₆]³⁻) as the electrocatalyst, repetitive application of an electrical potential to a solution containing static fibers formed by chemical oxidation by H_2O_2 did not cause any appreciable change to the fluorescence intensity (SI Movie 5), further confirming that the observed fluorescence changes in the full system were due to fiber assembly and disassembly, rather than simple electrochemical activation or physical attraction of the dye.

Active and Dynamic Self-Assembly. Next, we investigated active, dynamic self-assembly for the CSH/CSSC system

fueled by electricity. To observe the dynamics on a shorter time scale, we replaced DTT with a more efficient reductant, (tris(2-carboxyethyl)phosphine) (TCEP) 40 . The e-fueled system provides a convenient way to tune the kinetics of the reaction in real time by modulating the potential applied to the system. After applying an initial potential of 2 V vs. Ag/Ag $^{+}$ for 11 second to grow a layer of fibers from the electrode surface, the potential was reduced to 600 mV to slow down the fiber growth for observing dynamics at the fiber front. The CLSM video shows highly complex active, dynamic processes for the system (SI Movie 6), especially at the fiber–water interface (Fig. 3a,b). The selected snapshots highlight different modes of activity for the self-

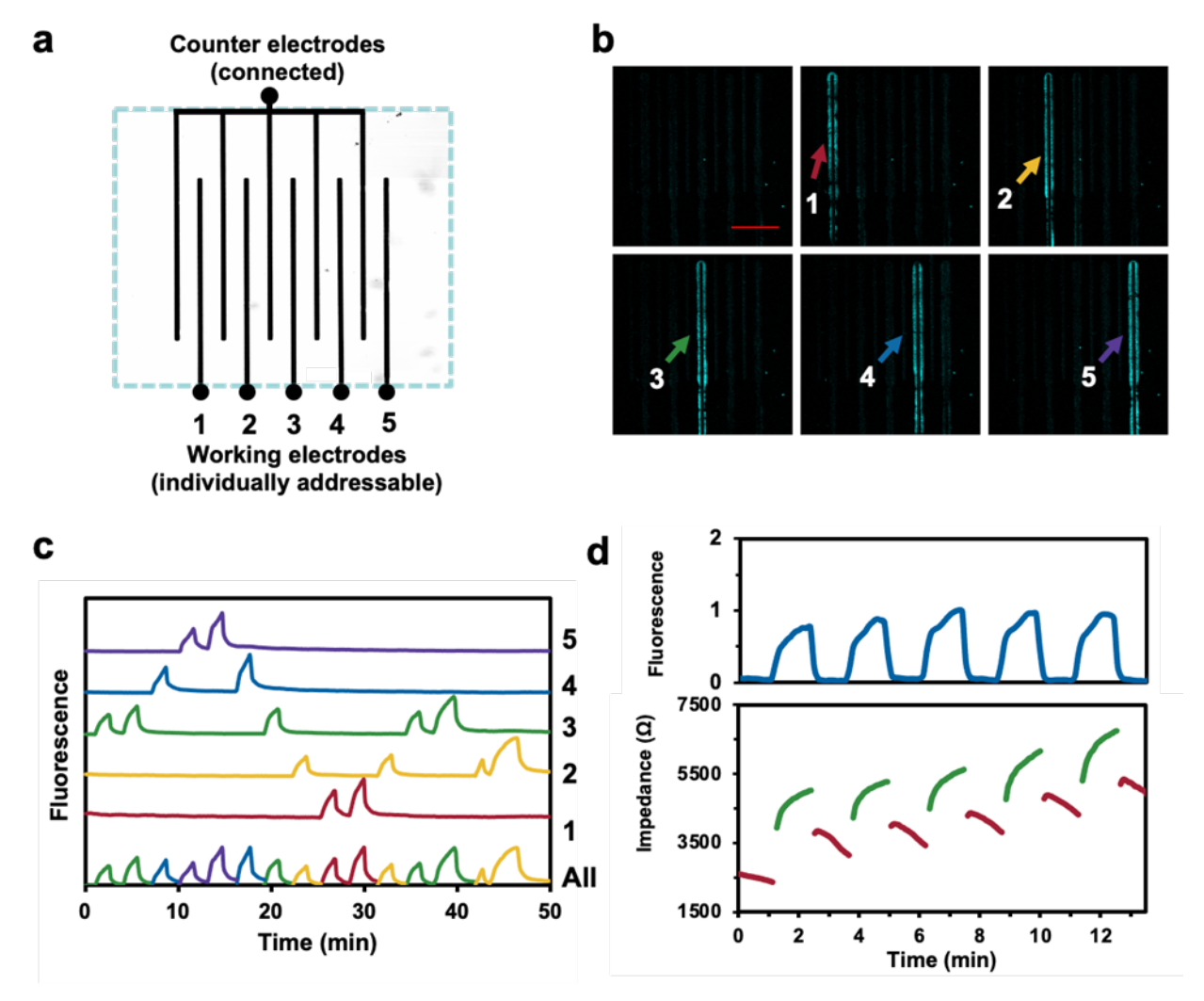


Figure 4. Spatiotemporal control of e-fueled dissipative assembly. (a) Schematic representation of the individually addressable interdigitated gold microelectrodes. (b) Growth of fibers at each of the working electrodes in a by selectively applying electric potential at different times (CLSM images rendered at 150 % hue saturation). (c) Normalized fluorescence intensity measured around each working electrode to monitor fiber growth pattern after selectively applying electric potential to each electrode at different times for varying durations. Each line corresponds to the working electrode of matching number and colour in b. The bottom trace superimposes 1-5 into one. If placed on a treble staff with the red graph at middle C, the pattern mimics that of the first four measures of Beethoven's "Ode to Joy" (see Fig. S7 and SI Movie 8). (d) Fluorescence and impedance changes in the system upon cycling fiber growth at 2.4 V and fiber dissolution at 0 V over 5 cycles.

assembly of fibers, including simultaneously growing and shrinking (Fig. 3c), waving (Fig. 3d), and curling and looping (Fig. 3e). Another observation is that as new fibers form at the front they collapse onto the body of the fibers already formed (SI Movie 6). The complexity of the observed active

behavior is tentatively attributed to multiple processes potentially ongoing in the system. In addition to the anticipated dissipative assembly/disassembly, several physicochemical processes may influence the active behavior. The electrochemical reaction should create concentration

gradients for both the redox-sensitive species and electrolytes near the working electrode surface (Fig. 1b), which may cause liquid-liquid phase separation of the growing fibers into a gel phase⁴¹. In addition, various electrostrictive hydrodynamics, such as electrohydrodynamics and/or electro-osmosis^{42,43}, may also contribute to the complex dynamic behavior. A control experiment without DTT in the solution (SI Movie 3) showed only static fiber formation without any of the dynamics observed in the active system, confirming that the observed dynamic behavior is indeed due to the dissipative self-assembly process.

The self-assembly dynamics observed in CLSM (SI Movie 6) were quantified using the structural dissimilarity index measurement (DSSIM) (Fig. 3b, f)44. DSSIM is a standard measure of the difference between two images, which compares variation in the mean, variance, and cross-correlation between local regions of two images (see SI for details). DSSIM images were obtained by comparing two frames taken 90 seconds (Fig. 3b, S9, SI Movie 7) or 4 seconds (Fig. S9-10, SI Movie 7) apart in a sliding-window calculation. The 90 second sliding-window calculation quantifies dynamics occurring over a large time window while the 4 seconds sliding-window calculation captures the high temporal resolution dynamics. Each of the 240 DSSIM images were divided into five equally spaced regions with increasing distance from the working electrode, and the average DSSIM in each region is plotted for every frame (Fig. 3f, Fig. S10d, SI Movie 7).

The results show that the dissipative self-assembly system is highly dynamic with the most dynamic changes at the fiber-water interface which is seen for both the 90 seconds and 4 seconds intervals. The dynamics decrease with distance from the fiber front, as can be seen with the time-delayed decline in DSSIM values starting with the 0-25 μm region which is then echoed in the 25-50 and 50-75 μm regions. The 75-100 and 100-125 μm regions start with low DSSIM values which steadily increase as the fiber-water interface progresses further from the electrode until a peak is reached, and then gradually decline. The data also shows that the dynamics at the fiber-water interface are highest in the early stages and gradually decrease over time.

Spatiotemporal Control of Active Assembly. Spatiotemporal control is a hallmark of biological dissipative self-assembly systems which is critical for their emergent functions^{1,2}. To demonstrate spatiotemporal control of the efueled active material system, we designed an array of interdigitated gold microelectrodes for use in a two-electrode configuration (Fig. 4a and Fig. S2). Each of the five bottom electrodes are individually addressable working electrodes, whereas the top five are connected as a single counter/reference electrode. By placing the sample solution (2.5 mM) CSH, 150 mM ferrocyanide, 60 mM DTT, pH 8 buffer) on the interdigitated microelectrodes and applying 2.4 V vs. ref for 90 seconds, fibers were grown at each individually addressed electrode (Fig. 4b). When the current was turned off, it took roughly 90 seconds to fully dissolve the fibers and return to baseline fluorescence. By selectively applying electric potential to different working electrodes over time, while also varying the duration for current on and off, the first four measures of Beethoven's "Ode to Joy" were "played" on the microelectrode array (Fig. 4c, Fig. S7, SI

Movie 8). This experiment clearly demonstrates precise spatiotemporal control and fast assembly/disassembly kinetics for the e-fueled dissipative system.

We also demonstrated that the e-fueled dissipative self-assemblies could dynamically transduce electronic inputs related to sensing, actuation, and computation. Single-frequency electrochemical impedance spectroscopy (SFEIS) was used to probe the impedance changes of the e-fueled dissipative assembly system on carbon-coated interdigitated gold microelectrodes (Fig. S2) at 8 kHz. The impedance of the system increased sharply upon application of 2.4 V ± 10 mV vs. ref for one minute, resulting from the growth of fiber networks between electrodes, and dropped after the potential was returned to 0 V ± 10 mV vs. ref (Fig. 4d). The fiber growth was concurrently monitored using CLSM during SFEIS measurements, confirming that the impedance changes correlate with fiber assembly and disassembly as indicated by changes in fluorescence intensity (Fig. 4d). In contrast, the control system without CSH in the solution only showed minimal changes of impedance under identical conditions (Fig. S13). The increase in impedance is attributed to the inhibition of ionic currents between electrodes due to diminished ionic transport through the selfassembled fiber network.

Conclusion and Outlook. In summary, here we have demonstrated a new platform for dissipative self-assembly of active materials by using an electric current as the fuel. Electrical inputs are able to rapidly and repetitively fuel the dissipative self-assembly of fibers with directionality, high dynamics, and precise spatiotemporal control. These combined features would be difficult to be achieved with either chemical or light fueled dissipative systems. Furthermore, the system operates in mild aqueous buffers, uses electrical energy as a clean fuel and works at relatively low voltage. These features make this design potentially suitable for developing sustainable dissipative self-assembly systems as well as applying this design to other redox sensitive assembling building blocks and/or microelectrode arrays. Currently, we are working towards a complete electrically fueled dissipative self-assembly system where both oxidation and reduction proceed electrochemically, with the aim to achieve a waste-free and sustainable dissipative self-assembly system for further study. As electronic signals are at the heart of many modern technologies, the described efueled active material platform may find potential applications in bioelectronics. 45,46

ASSOCIATED CONTENT

Supporting Information

The Supporting Information is available free of charge on the ACS Publications website.

Materials, electrode design, experimental details and data for confocal laser scanning microscopy, kinetic data, DSSIM process and characterization, rheology data, cryo-TEM characterization. (PDF)

SI Movie 1. Video depicting the transient growth and disassembly of the e-fueled supramolecular fibers. Accompanies Figure 2. (MP4)

- SI Movie 2. Video depicting the growth of gel upon continuous application of a 600 mV electrical potential. The stage is moved throughout the experiment to follow the gel growth. (MP4)
- SI Movie 3. Video depicting the growth of gel in the absence of reductant. (MP4)
- SI Movie 4. Video depicting the repeated application of an electrical potential to a sample which lacks the redox active CSH building block precursor. (MP4)
- SI Movie 5. Video depicting the repeated application of an electrical potential to a sample of chemically grown gel fibers in the absence of both reductant and electrochemical mediator ferrocyanide. (MP4)
- SI Movie 6. Video depicting the active dynamic behavior of the e-fueled dissipative self-assembly fibers. Accompanies Fig. 3. (MP4)
- SI Movie 7. Realtime generation of DSSIM plots based on 90 s and 4 s sliding-window calculations. Accompanies Fig. 3. (MP4)
- SI Movie 8. Spatiotemporally controlled dissipative self-assembly of fibers at an interdigitated gold microelectrode junction synced with the tune of Beethoven's "Ode to Joy." Accompanies Fig. 4. (MP4)

AUTHOR INFORMATION

Corresponding Author

* zguan@uci.edu

ORCID^{ID}

Zhibin Guan: 0000-0003-1370-1511

Funding Sources

This work was financially supported by the US Department of Energy, Office of Science, Basic Energy Sciences (DE-FG02-04ER46162; Z.G.; initial demonstration of e-fueled dissipative self-assembly in bulk solution) and the National Science Foundation Materials Research Science and Engineering Center program through the UC Irvine Center for Complex and Active Materials (DMR-2011967; Z.G., A.I.H., J.P.P., R.R.; demonstration of e-fueled self-assembly on microelectrodes and comprehensive characterizations of e-fueled dissipative systems by CLSM, cryo-TEM, DSSIM analysis, and electrochemical impedance spectroscopy), with partial support from the National Science Foundation (CHE-1904939; Z.G.; kinetic study).

Notes

The authors declare not competing financial interests.

ACKNOWLEDGMENT

The authors also acknowledge the use of facilities and instrumentation at the UC Irvine Materials Research Institute (IMRI) supported in part by the National Science Foundation Materials Research Science and Engineering Center program through the UC Irvine Center for Complex and Active Materials (DMR-2011967). H.W. acknowledges the use of facilities and instrumentation at the Integrated Nanosystems Research Facility (INRF) in the Samueli School of Engineering at the University of California Irvine. This study was made possible in part through access to the Optical Biology Core Facility of the Developmental Biology Center, a shared resource supported by the

Cancer Center Support Grant (CA-62203) and Center for Complex Biological Systems Support Grant (GM-076516) at the University of California, Irvine. S.S. acknowledges support by an NSERC postdoctoral fellowship from the Research Council of Canada. J.T.M. acknowledges the donors of The American Chemical Society Petroleum Research Fund. The authors thank Shane Ardo and Jenny Yang for help with electrochemical studies.

REFERENCES

- (1) Alberts, B.; Johnson, A.; Lewis, J.; Raff, M.; Roberts, K.; Walter, P. *Molecular Biology of the Cell, 4th Edition*; Garland Science, 2002.
- (2) Fletcher, D. A.; Geissler, P. L. Active biological materials. *Annu. Rev. Phys. Chem.* **2009**, *60*, 469-486. DOI: 10.1146/annurev.physchem.040808.090304.
- (3) Nicolis, G.; Prigogine, I. *Self-Organization in Nonequilibrium Systems: From Dissipative Structures to Order Through Fluctuations*; John Wiley & Sons, 1977.
- (4) Boekhoven, J.; Hendriksen, W. E.; Koper, G. J. M.; Eelkema, R.; van Esch, J. H.; Transient assembly of active materials fueled by a chemical reaction. *Science.* **2015**, *349*, 1075-1079. DOI: 10.1126/science.aac6103.
- (5) Riess, B.; Groetsch, R. K.; Boekhoven, J. The Design of Dissipative Molecular Assemblies Driven by Chemical Reaction Cycles. *Chem* **2020**, *6*, 552-578. DOI: 10.1016/j.chempr.2019.11.008.
- (6) Das, K.; Gabrielli, L.; Prins, L. J.; Chemically Fueled Self-Assembly in Biology and Chemistry. *Angew. Chem., Int. Ed.* **2021**, *60*, 20120-20143. DOI: 10.1002/anie.202100274.
- (7) Mattia, E.; Otto, S. Supramolecular systems chemistry. *Nat. Nanotechnol.* **2015**, *10*, 111-119. DOI: 10.1038/nnano.2014.337 (2015).
- (8) Klajn, R.; Wesson, P. J.; Bishop, K. J. M; Grzybowski, B. A. Writing Self-Erasing Images using Metastable Nanoparticle "Inks". *Angew. Chem., Int. Ed.* **2009**, *48*, 7035-7039. DOI: 10.1002/anie.200901119.
- (9) Ross, T. D.; Lee, H. J.; Qu, Z.; Banks, R. A.; Philips, R.; Thomson, M. Controlling organization and forces in active matter through optically defined boundaries. *Nature.* **2019**, *572*, 224-229. DOI: 10.1038/s41586-019-1447-1.
- (10) Weissenfels, M.; Gemen, J.; Klajn, R. Dissipative Self-Assembly: Fueling with Chemicals versus Light. *Chem.* **2017**, *7*, 23-37. DOI: 10.1016/j.chempr.2020.11.025.
- (11) Tena-Solsona, M.; Rieβ B.; Grötsch, R. K.; Löhrer, F. C.; Wanzke, C.; Käsdorf, B.; Bausch, A. R.; Müller-Buschbaum, P.; Lieleg, O.; Boekhoven, J. Non-equilibrium dissipative supramolecular materials with a tunable lifetime. *Nat. Commun.* **2017**, *8*, 15895. DOI: 10.1038/ncomms15895.
- (12) Kariyawasam, L. S.; Hartley, C. S. Dissipative Assembly of Aqueous Carboxylic Acid Anhydrides Fueled by Carbodiimides. *J. Am. Chem. Soc.* **2017**, *139*, 11949-11955. DOI: 10.1021/jacs.7b06099.
- (13) Sorrenti, A.; Leira-Iglesias, J.; Sato, A.; Hermans Thomas, M. Non-equilibrium steady states in supramolecular polymerization. *Nat. Commun.* **2017**, *8*, 15899. DOI: 10.1038/ncomms15899
- (14) Maiti, S.; Fortunati, I.; Ferrante, C.; Scrimin, P.; Prins, L. J. Dissipative self-assembly of vesicular nanoreactors. *Nat. Chem.* **2016**, *8*, 725-731. DOI: 10.1038/nchem.2511.
- (15) Mishra, A.; Korlepara, D. B.; Kumar, M.; Jain, A.; Jonnalagadda, N.; Bejagam, K. K.; Balasubramanian S.; George, S. J. Biomimetic temporal self-assembly via fuel-driven controlled supramolecular polymerization. *Nat. Commun.* **2018**, *9*, 1-9. DOI: 10.1038/s41467-018-03542-z.
- (16) te Brinke, E.; Groen, J.; Herrmann, A.; Heus, H. A.; Rivas, G.; Spruijt, E.; Huck, W. T. S. Dissipative adaptation in driven self-assembly leading to self-dividing fibrils. *Nat. Nanotechnol.* **2018**, *13*, 849-855. DOI: 10.1038/s41565-018-0192-1.

- (17) Heinen, L.; Walther, A. Programmable dynamic steady states in ATP-driven nonequilibrium DNA systems. *Sci. Adv.* **2019**, *5*, eaaw0590, DOI: 10.1126/sciadv.aaw0590.
- (18) Leira-Iglesias, J.; Tassoni, A.; Adachi, T.; Stich, M.; Hermans, T. M. Oscillations, travelling fronts and patterns in a supramolecular system. *Nat. Nanotechnol.* **2018**, *13*, 1021-1027. DOI: 10.1038/s41565-018-0270-4.
- (19) Ogden, W. A.; Guan, Z. Redox Chemical-Fueled Dissipative Self-Assembly of Active Materials. *ChemSystemsChem.* **2020**, *2*, e1900030, DOI: 10.1002/syst.201900030.
- (20) Colomer, I.; Morrow Sarah, M.; Fletcher Stephen, P. A transient self-assembling self-replicator. *Nat. Commun.* **2018**, *9*, 2239. DOI: 10.1038/s41467-018-04670-2.
- (21) Bal, S.; Das, K.; Ahmed, S.; Das, D. Chemically Fueled Dissipative Self-Assembly that Exploits Cooperative Catalysis. *Angew. Chem., Int. Ed.* **2019**, *58*, 244-247. DOI: 10.1002/anie.201811749.
- (22) Debnath, S.; Roy, S.; Ulijn, R. V. Peptide Nanofibers with Dynamic Instability through Nonequilibrium Biocatalytic Assembly. *J. Am. Chem. Soc.* **2013**, *135*, 16789-16792. DOI: 10.1021/ja4086353.
- (23) Kubota, R.; Makuta, M.; Suzuki, R.; Ichikawa, M.; Tanaka, M.; Hamachi, I. Force generation by a propagating wave of supramolecular nanofibers. *Nat. Commun.* **2020**, *11*, 3541. DOI: 10.1038/s41467-020-17394-z.
- (24) Del Grosso, E.; Prins, L. J.; Ricci, F. Transient DNA-Based Nanostructures Controlled by Redox Inputs. *Angew. Chem., Int. Ed.* **2020**, *59*, 13238-13245. DOI: 10.1002/anie.202002180.
- (25) Groetsch, R. K.; Wanzke, C.; Speckbacher, M.; Angi, A.; Rieger, B.; Boekhoven, J. Pathway Dependence in the Fuel-Driven Dissipative Self-Assembly of Nanoparticles. *J. Am. Chem. Soc.* **2019**, *141*, 9872-9878. DOI: 10.1021/jacs.9b02004.
- (26) Ikegami, T.; Kageyama, Y.; Obara, K.; Takeda, S. Dissipative and Autonomous Square-Wave Self-Oscillation of a Macroscopic Hybrid Self-Assembly under Continuous Light Irradiation. *Angew. Chem., Int. Ed.* **2016**, *55*, 8239-8243. DOI: 10.1002/anie.201600218.
- (27) de Jong, J. J. D.; Hania, P. R.; Pugžlys, A.; Lucas, L. N.; de Loos, M.; Kellogg, R. M.; Feringa, B. L.; Duppen, K.; van Esch, J. H. Lightdriven dynamic pattern formation. *Angew. Chem., Int. Ed.* **2005**, *44*, 2373-2376. DOI: 10.1002/anie.200462500.
- (28) Klajn, R.; Bishop, K. J. M.; Grzybowski, B. A. Light-controlled self-assembly of reversible and irreversible nanoparticle suprastructures. *Proc. Natl. Acad. Sci. U. S. A.* **2007**, *104*, 10305-10309. DOI: 10.1073/pnas.0611371104.
- (29) Bar-Cohen, Y. *Electroactive Polymer (EAP) Actuators as Artificial Muscles: Reality, Potential, and Challenges, Second Edition*; SPIE PRESS, 2004.
- (30) Woltman, S. J.; Jay, G. D.; Crawford, G. P. Liquid-crystal materials find a new order in biomedical applications. *Nat. Mater.* **2007**, *6*, 929-938. DOI: 10.1038/nmat2010.
- (31) Yeh, S.-R.; Seul, M.; Shraiman Boris, I. Assembly of ordered colloidal aggregates by electric-field-induced fluid flow. *Nature*. **1997**, *386*, 57-59. DOI: 10.1038/386057a0.
- (32) Ma, F.; Yang, X.; Zhao, H.; Wu, N. Inducing propulsion of colloidal dimers by breaking the symmetry in electrohydrodynamic flow. *Phys. Rev. Lett.* **2015**, *115*, 208302. DOI: 10.1103/PhysRevLett.115.208302.

- (33) Electropolymerization: Concepts, Materials And Applications; Cosnier, S.; Karyakin, A.; Eds.; Wiley, 2010. DOI: 10.1002/9783527630592.
- (34) Ellis, T. K.; Galerne, M.; Armao, J. J. IV; Osypenko, A.; Martel, D.; Maaloum, M.; Fuks, D.; Gavat, O.; Moulin, E.; Giuseppone, N. Supramolecular Electropolymerization. *Angew. Chem., Int. Ed.* **2018**, *57*, 15749-15753. DOI: 10.1002/anie.201809756.
- (35) Chen, S.; Itoh, S.; Masuda, T.; Shimizu, S.; Zhao, J.; Ma, J.; Nakamura, S.; Okuro, K.; Noguchi, H.; Uosaki, K.; Aida, T. Subnanoscale hydrophobic modulation of salt bridges in aqueous media. *Science*. **2015**, *348*, 555-559. DOI: 10.1126/science.aaa7532.
- (36) Krabbenborg, S. O.; Veerbeek, J.; Huskens, J. Spatially Controlled Out-of-Equilibrium Host-Guest System under Electrochemical Control. *Chem. Eur. J.* **2015**, *21*, 9638-9644. DOI: 10.1002/chem.201501544.
- (37) Gortner, R. A.; Hoffman, W. F. An Interesting Colloid Gel. *J. Am. Chem. Soc.* **1921**, *43*, 3. DOI: 10.1021/ja01443a009.
- (38) Tschirhart, T.; Kim, E.; McKay, R.; Ueda, H.; Wu, H.-C.; Pottash, A. E.; Zargar, A.; Negrete, A.; Shiloach, J.; Payne, G. F.; Bently, W. E. Electronic control of gene expression and cell behaviour in Escherichia coli through redox signalling. *Nat. Commun.* **2017**, *8*, 14030. DOI: 10.1038/ncomms14030.
- (39) Nekrassova, O.; Allen, G. D.; Lawrence, N. S.; Jiang, L.; Jones, T. G. J.; Compton, R. G. The oxidation of cysteine by aqueous ferricyanide: a kinetic study using boron doped diamond electrode voltammetry. *Electroanalysis.* **2002**, *14*, 1464-1469. DOI: 10.1002/1521-4109(200211)14:21<1464::Aid-elan1464>3.0.Co;2-o.
- (40) Burns, J. A.; Butler, J. C.; Moran, J.; Whitesides, G. M. Selective reduction of disulfides by tris(2-carboxyethyl)phosphine. *J. Org. Chem.* **1991**, *56*, 2648-2650. DOI: 10.1021/jo00008a014.
- (41) Saini, S.; Bukosky, S. C.; Ristenpart, W. D. Influence of Electrolyte Concentration on the Aggregation of Colloidal Particles near Electrodes in Oscillatory Fields. *Langmuir.* **2016**, *32*, 4210-4216. DOI: 10.1021/acs.langmuir.5b04636.
- (42) Ristenpart, W. D.; Jiang, P.; Slowik, M. A.; Punckt, C.; Saville, D. A.; Aksay, I. A. Electrohydrodynamic Flow and Colloidal Patterning near Inhomogeneities on Electrodes. *Langmuir.* **2008**, *24*, 12172-12180. DOI: 10.1021/la801419k.
- (43) Davidson S. M.; Andersen M. B.; Mani, A. Chaotic induced-charge electro-osmosis. *Phys. Rev. Lett.* **2014**, *112*, 128302. DOI: 10.1103/PhysRevLett.112.128302.
- (44) Wang, Z.; Bovik A. C.; Sheikh H. R.; Simoncelli E. P. Image quality assessment: from error visibility to structural similarity. *IEEE transactions on image processing.* **2004**, *13*, 600-612. DOI: 10.1109/TIP.2003.819861.
- (45) Song, E.; Li, J.; Won, S. M.; Bai, W.; Rogers, J. A. Materials for flexible bioelectronic systems as chronic neural interfaces. *Nat. Mater.* **2020**, *19*, 590-603. DOI: 10.1038/s41563-020-0679-7.
- (46) Liu, Y.; Li, J.; Song, S.; Kang, J.; Tsao, Y.; Chen, S.; Mottini, V.; McConnell, K.; Xu, W.; Zheng, Y.-Q.; Tok, J. B.-H.; George, P. M.; Bao, Z. Morphing electronics enable neuromodulation in growing tissue. *Nat. Biotechnol.* **2020**, *38*, 1031-1036. DOI: 10.1038/s41587-020-0495-2.

Table of Contents Figure:

